

## Transport Improvement Near Low Order Rational $q$ Surfaces in DIII-D

M.E. Austin 1), K.H. Burrell 2), R.E. Waltz 2), K.W. Gentle 1), P. Gohil 2),  
 C.M. Greenfield 2), R.J. Groebner 2), W.W. Heidbrink 3), Y. Luo 3), J.E. Kinsey 4),  
 M.A. Makowski 5), G.R. McKee 6), R. Nazikian 7), C.C. Petty 2), R. Prater 2),  
 T.L. Rhodes 8), M.W. Shafer 6), and M.A. VanZeeland 9)

- 1) University of Texas-Austin, Austin, Texas, USA
- 2) General Atomics, San Diego, California 92186-5608, USA
- 3) University of California-Irvine, Irvine, California 92697, USA
- 4) Lehigh University, Bethlehem, Pennsylvania, USA
- 5) Lawrence Livermore National Laboratory, Livermore, California, USA
- 6) University of Wisconsin-Madison, Madison, Wisconsin 53706, USA
- 7) Princeton Plasma Physics Laboratory, Princeton, New Jersey, USA
- 8) University of California-Los Angeles, Los Angeles, California, USA
- 9) Oak Ridge Institute for Science Education, Oak Ridge, Tennessee, USA

e-mail contact of main author: austin@fusion.gat.com

**Abstract.** Detailed measurements of transient variations of kinetic profiles and turbulence levels in DIII-D negative central shear plasmas have led to a model for transport changes near integer  $q_{\min}$  crossings based on the effects of zonal flow structures. In particular the timing and amplitude of  $T_e$  gradient changes near  $q_{\min} = 2$  match predictions of the temperature component of the zonal flow structures obtained from nonlinear GYRO simulations. Also, the observation of fluctuation level reductions and poloidal turbulence velocity increases are consistent with the modeling. The interplay of zonal-flow-induced ExB shear and ExB shear from equilibrium rotation provides an explanation for the power threshold for the formation of sustained core transport barriers.

### 1. Introduction

As fusion energy research progresses to burning plasma experiments, it will be important to understand how to access regimes of improved confinement. In many magnetic fusion devices, improvements in transport have been observed near low-order rational  $q$  surfaces, often leading to the formation of internal transport barriers. Experiments to advance the physics understanding of this phenomenon have been performed in DIII-D by examining closely the timing and spatial structure of the transport changes near integer  $q$ .

DIII-D [1] and other tokamaks [2-8] have seen a connection between low-order rational surfaces, particularly  $q = 2$  surfaces, and internal transport barrier (ITB) formation. For most of these cases the changes in transport are observed in discharges with reverse or negative shear in the core meaning that the  $q$  profile has a minimum value,  $q_{\min}$ , that is off-axis and the second derivative is small there. The changes in transport occur near the time when  $q_{\min}$  crosses an integer or half-integer value. Explanations for these transport changes have invoked “good surfaces” near low-order rational values of  $q$  without a specific explanation of what makes the surfaces good. In this paper we present experimental observations of  $T_e$ ,  $T_i$ ,  $v_\phi$ , and fluctuation measurements that qualitatively match predictions from GYRO code simulations, which in turn suggest a seminal role in zonal flow structures near the rational surface causing the transport reduction.

### 2. Transport Changes Near Integer $q_{\min}$

In DIII-D, the effects of crossing integer  $q$  values are most readily seen in low density, neutral beam heated, L-mode, negative central shear (NCS) discharges where  $q_{\min}$  is typically at the

half radius,  $r/a \sim 0.5$ . In these discharges, transient or enduring increases in ion and electron temperature are observed as  $q_{\min}$  traverses integer values as shown in Fig. 1. At the  $q_{\min} = 2$  crossing an internal transport barrier forms for the ions in this discharge with the neutral beam injected power at 5 MW. At higher powers in this type of discharge, ITBs tend to form independent of integer  $q$  values; at lower powers, only transient confinement improvements occur near the integer  $q_{\min}$  crossings.

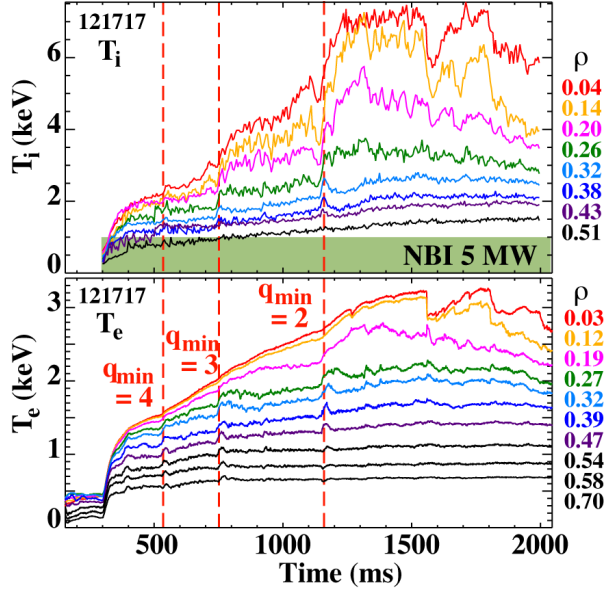


FIG. 1. Ion and electron temperature time traces for a typical NCS ITB shot ( $I_p = 1.2$  MA,  $B_T = 2.0$  T). The  $q =$  integer times are determined from motional Stark effect (MSE)-constrained EFIT reconstructions and RSAE modes. The ITB is triggered at 1150 ms for 5 MW of NB power. The drop in central temperatures at 1550 ms is caused by the onset of a core MHD mode.

The timing of the transport changes relative to the appearance of the rational surface has been measured carefully in DIII-D experiments and is key to understanding the underlying physics. The evolution of the  $q$  profile is determined accurately with a combination of MSE-constrained EFITs and observation of reverse shear Alfvén eigenmodes (RSAE) [9] as shown in Fig. 2. The spectrogram of  $n_e$  fluctuations from the FIR scattering diagnostic shows a multitude of coherent modes chirping up in frequency; these are the RSAE. The “grand cascade,” a group of upchirping modes that start simultaneously at the time  $q_{\min} = \text{integer}$ , is seen at 1150 ms and this marks unambiguously the  $q_{\min} = 2$  time. The  $q$  profiles from EFIT reconstructions have uncertainties that make it difficult to ascertain  $q_{\min} = \text{integer}$  times to better than 20 ms; using the grand cascades, the times of integer  $q_{\min}$  crossings can be resolved to within 2 ms.

The transport changes can be closely followed by observing the  $T_e$  gradient evolution using pairs of adjacent ECE channels. The measurements show that the temperature gradient increase begins 5-20 ms before the crossing of  $q_{\min} = \text{integer}$ , and for the case of a transient change in transport, the elevated gradient remains for a comparable interval afterwards. A typical example of the  $T_e$  gradient changes around  $q_{\min} = 2$  is shown in Fig. 3(a) with the gradient amplitude expressed in terms of  $a/L_{T_e} = (a/T_e)dT_e/dR$ .

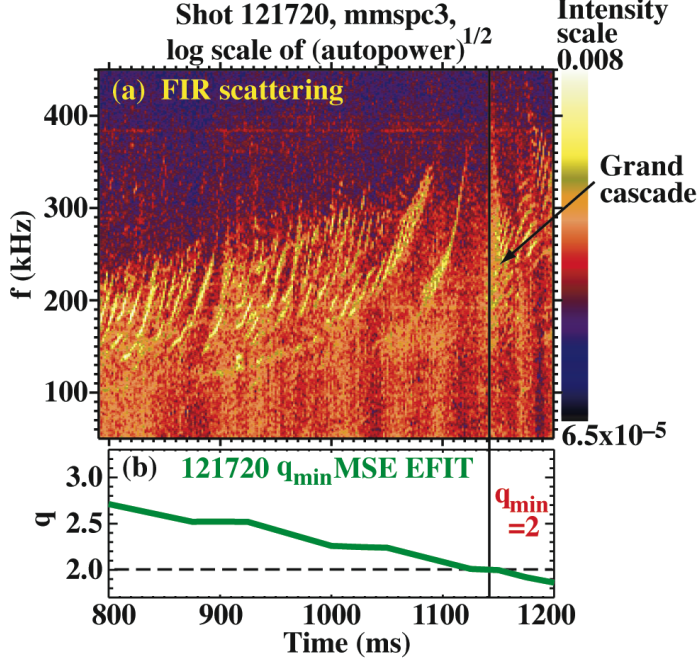


FIG. 2. (a) Spectrogram of FIR scattering low- $k$  ( $k_\theta \sim 0\text{--}1 \text{ cm}^{-1}$ ) data showing RSAE modes and the grand cascade that begins at  $q_{\min} = 2$  for discharge 121720. (b)  $q_{\min}(t)$  derived from MSE EFITs.

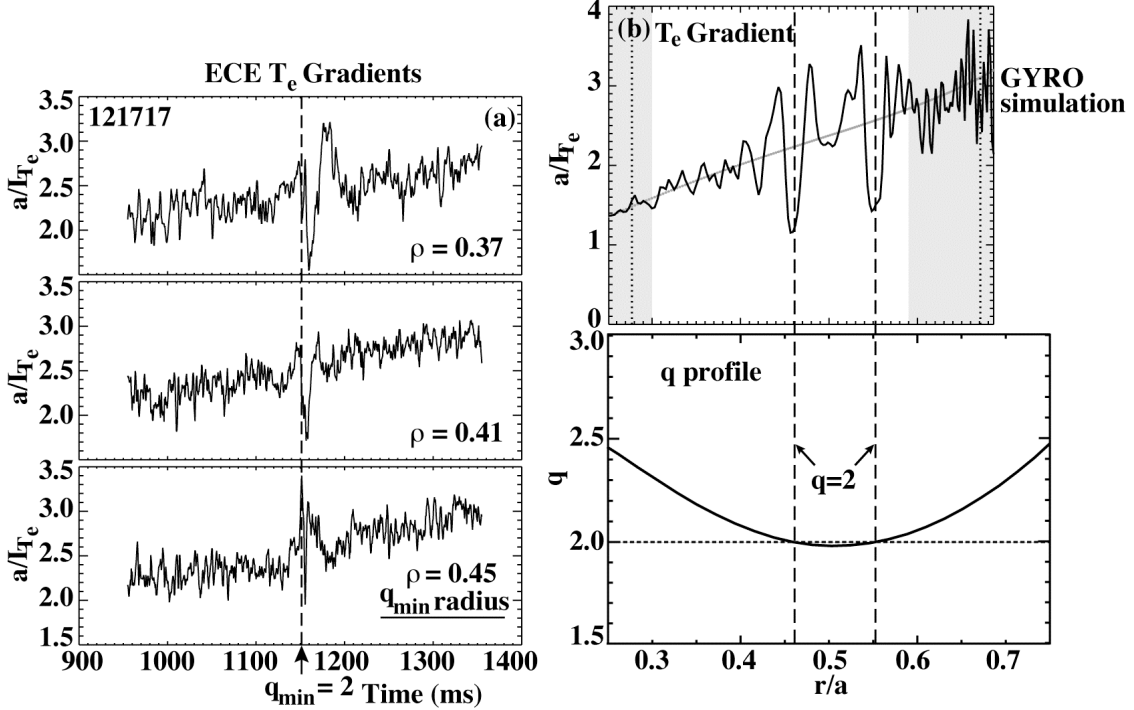


FIG. 3. (a)  $\nabla T_e(t)$  around the  $q_{\min} = 2$  time for three locations near the  $q_{\min}$  radius for the two-NB-source shot of Fig. 1. (b)  $T_e$  gradient versus normalized radius from a GYRO code simulation using the plasma conditions from shot 121717 at 1155 ms and the  $q$  profile for this timeslice.

One implication of the timing of the temperature increases is that the transport changes are not caused by the effects of magnetic reconnection since the changes occur before the integer  $q$  surface comes into the plasma. Also, in discharges with low heating power, no low frequency mode activity is seen in the magnetic probe signals near the time of integer  $q$ . High frequency modes, such as fast ion driven Alfvén eigenmodes, are not believed to be playing a role because in discharges with no measurable fast ion mode activity the electron temperature behavior is the same.

### 3. Comparison with GYRO Code Simulations

The measured  $T_e$  gradient evolution displayed in Fig. 3(a) is in agreement with physically comprehensive GYRO code simulations predicting profile corrugations near low-order rational  $q$  surfaces [10]. These profile corrugations are zonal flow structures that occur due to the gap in rational surfaces near integer  $q$ . They are expected to be large for the case of strong turbulence and negative central shear as in the DIII-D experiments. Simulation results for shot 121717 at the time when  $q_{\min}$  is just below 2 are given in Fig. 3(b), and this shows the typical result that the time averaged gradient profile exhibits a steepening on either side of  $q_{\min}$ , and a flattening right at  $q_{\min}$ . In the experiment, the  $q$  profile is continually evolving; this is essentially equivalent to traversing the profile in Fig. 3(b) from left to right and one would expect to see in time the gradient steepening, flattening, then steepening again, as is indeed the case in Fig. 3(a).

To further test the GYRO predictions versus experiment, a set of simulations were run with the same input profiles but with the  $q$  profile modified to have  $q_{\min}$  3% above 2, 0.5% above 2 and at 2 minus epsilon. The case at  $q_{\min} = 2.06$  shows no corrugations. The results for the second and third cases are shown in Fig. 4 where there are some signs that the  $T_e$  gradient has begun to steepen at the  $q_{\min}$  radius when  $q_{\min} = 2.01$  and then drops sharply when  $q_{\min} = 2.00(-)$ , the same as seen in the experiment. More details of these GYRO runs are provided in Ref. [11].

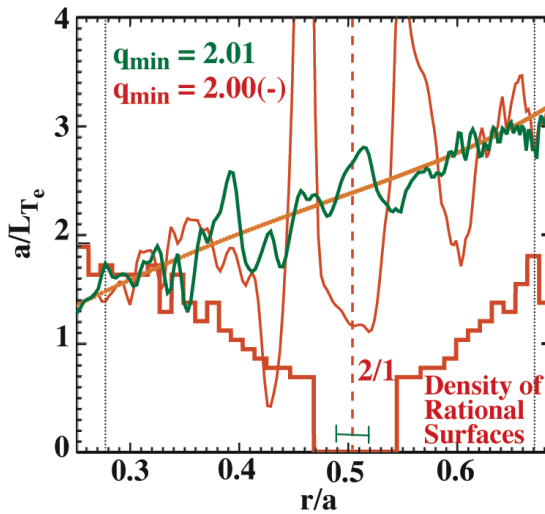


FIG. 4.  $T_e$  gradients from GYRO simulations using negative central shear  $q$  profiles with  $q_{\min}$  just above and just below 2.

#### 4. Turbulent Fluctuation Measurements

GYRO predicts a large zonal flow ExB shear layer associated with the  $q_{\min} = 2$  profile corrugations. This shear layer should have a significant effect on turbulence near the integer  $q_{\min}$  time. In fact, we have seen evidence of both a large shear layer and a decrease of turbulent fluctuations in these DIII-D discharges as the integer  $q$  values are crossed. Figure 5 shows transient reductions in low- $k$  turbulent fluctuation levels as measured by the beam emission spectroscopy (BES) diagnostic in a shot similar to the discharge in Fig. 1. Figure 6 displays a localized burst in the poloidal velocity of the turbulence at the  $q_{\min}$  radius also detected with the BES system. We have also seen a decrease of intermediate  $k$  ( $\sim 7 \text{ cm}^{-1}$ ) fluctuations, measured by the FIR scattering diagnostic, starting at the  $q_{\min} = 2$  time and continuing throughout the core barrier phase. These observations are consistent with the zonal flow structure picture of transport reduction.

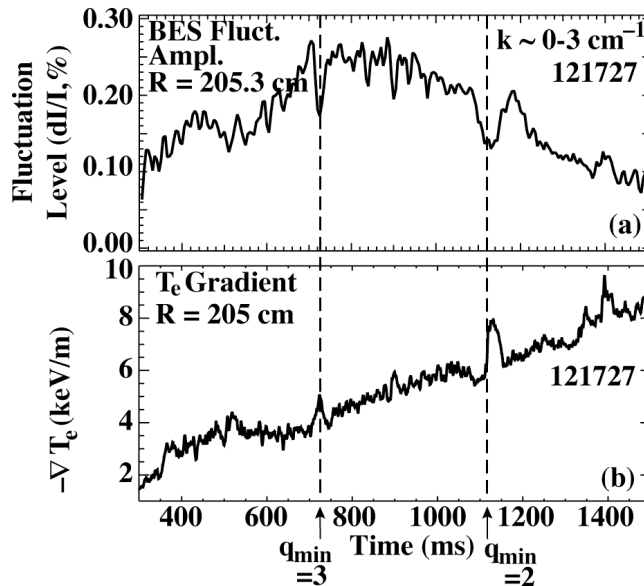


Fig. 5. (a) Fluctuation amplitude ( $\tilde{n}_e/n_e$ ) vs time from the BES diagnostic for a shot with confinement improvement at the time at  $q_{\min} = 3$  and  $q_{\min} = 2$  crossings. (b) Local  $T_e$  gradient versus time at the BES measurement radius. The radius of the  $q_{\min}$  is between 200-205 cm for this time window.

In a recent experiment in DIII-D, the equilibrium ExB rotational shear was varied by using different mixes of co and counter beams in NCS low density plasmas to determine the role of ExB shear and zonal flows in the formation of ITBs. With 100% co-injection, ITBs were initiated at  $q_{\min} = 2$  with 5 MW; at 7.5 MW signs of core barrier formation were evident before the  $q_{\min} = 2$  time. For balanced beam and partially counter-injected discharges, no ITBs formed but the transient zonal flow  $T_e$  gradient structures were still seen at the integer  $q_{\min}$  times, along with transient reductions in turbulent fluctuations. These results confirm the model that the confinement improvement due to zonal flows acts as a trigger for core barrier formation only if the background ExB shear is large enough.

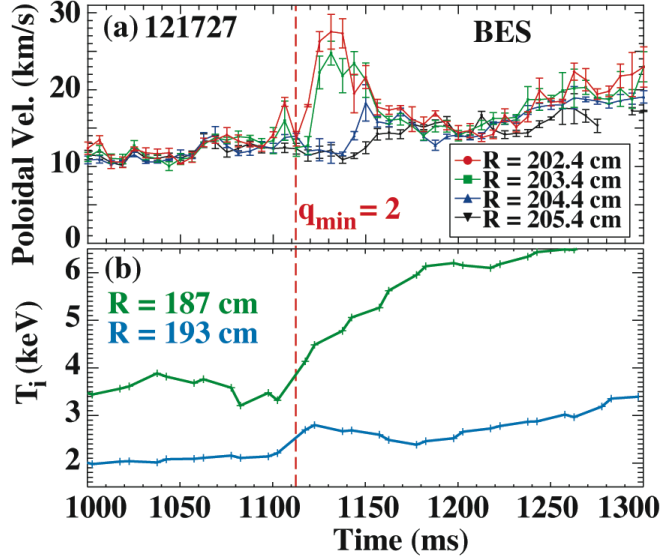


Fig. 6. (a) Poloidal velocity evolution derived from BES measurements near the  $q_{\min} = 2$  time for the same discharge as Fig. 5. (b) Core  $T_i$  versus time for two locations showing barrier formation at the  $q_{\min} = 2$  crossing.

## 5. Conclusions

We have observed changes in transport near integer  $q$  values in DIII-D NCS discharges. The changes can be transient or an enduring transport barrier can form depending on input power levels. We have developed a model for core barrier formation based on GYRO code results that predict profile corrugations in the vicinity of low-order rational  $q$  surfaces. The profile corrugations are a manifestation of zonal flow structures that have significant radial extent in the case of large flat shear regions in NCS discharges. In cases where the equilibrium ExB shear rotation is of a magnitude to make the discharge marginal for barrier formation, the zonal-flow-induced ExB shear that arises at integer  $q_{\min}$  is sufficient to push the discharge into a state of improved core confinement. The observations of  $T_e$  gradient structures, turbulence reductions, and increases in poloidal turbulence velocity near integer  $q$  are all in consistent with the concept of integer- $q$ -localized zonal flows.

This work was supported by the U.S. Department of Energy under DE-FG03-97ER54415, DE-FC02-04ER54698, SC-G903402, DE-FG02-92ER54141, W-7405-ENG-48, DE-FG02-89ER53296, DE-FG03-01ER54615, and DE-AC05-76OR00033.

## References

- [1] GREENFIELD, C.M., RETTIG, C.L., STAEBLER, G.M., *et al.*, Nucl. Fusion **39** (1999) 1723.
- [2] GÜNTER, S., *et al.*, Proc. of the 28th European Physical Society Conf. on Control. Fusion and Plasma Physics (Madeira, 2002) Vol 25A, P1.006.
- [3] KOIDE, Y., *et al.*, Phys. Rev. Lett. **72** (1994) 3662.

- [4] RAZUMOVA, K.A., *et al.*, Proc. of the 19th Int. Conf. on Fusion Energy (Lyon, 2002) (Vienna: IAEA), CD-ROM file IAEA-CN-94/EX/P3-03 and <http://www.iaea.org/programmes/ripc/physics/fec2002/html/fec2002.htm>.
- [5] BELL, M., *et al.*, Plasma Phys. Control. Fusion **41** (1999) A719.
- [6] HOGEWEIJ, G.M.D., LOPES CARDOZO, N.J., de BAAR, M.R., SCHILHAM, A.M.R., Nucl. Fusion **38** (1998) 1881.
- [7] de BAAR, M.R., BEURSKENS, M.N.A., HOGEWEIJ, G.M.D., LOPES CARDOZO, N.J., Phys. Plasmas **6** (1999) 4645.
- [8] JOFFRIN, E., GORINI, G., CHALLIS, C.D., HAWKES, N.C., HENDER, T.C., HOWELL, D.F., MAGET, P., MANTICA, P., MAZON, D., SHARAPOV, S.E., TRESSET, G., Plasma Phys. Control. Fusion **44** (2002) 1739.
- [9] SHARAPOV, S.E., ALPER, B., BERK, H.L., BORBA, D., Phys. Plasmas **9** (2002) 2027.
- [10] WALTZ, R.E., CANDY, J., HINTON, F.L., ESTRADA-MILA, C., KINSEY, J.E., Nucl. Fusion **45** (2005) 741.
- [11] WALTZ, R.E., AUSTIN, M.E., BURRELL, K.H., CANDY, J., Phys. Plasmas **13** (2006) 052301.